JOURNAL OF ENERGY SYSTEMS

2024, 8(2)

2602-2052 DOI: 10.30521/jes.1339832 Research Article

Online estimation of state-of-charge using auxiliary load

Abdelaziz Zermout
University M'hamed Bougara of Boumerdes, Institute of Electrical and Electronic Engineering, Signals and Systems Laboratory, Boumerdes 35000, Algeria, az.zermout@univ-boumerdes.dz

Hadjira Belaidi*
University M'hamed Bougara of Boumerdes, Institute of Electrical and Electronic Engineering, Signals and Systems Laboratory, Boumerdes 35000, Algeria, ha.belaidi@univ-boumerdes.dz

Ahmed Maache
University M'hamed Bougara of Boumerdes, Institute of Electrical and Electronic Engineering, Signals and Systems Laboratory, Boumerdes 35000, Algeria, a.maache@univ-boumerdes.dz

Submitted: 09.08.2023
Accepted: 07.03.2024
Published: 30.06.2024

* *Corresponding Author*

Abstract: Numerous approaches and methodologies have been established for online (while the load is supplied) estimation of the State-of-Charge of Lithium-ion cells and batteries. However, as battery load consumption fluctuates in real time because of delivered device operations, obtaining a precise online state of charge estimation remains a challenging task. This work proposes a new technique for online open circuit voltage measurement to estimate state of charge of batteries. This novel technique proposes the addition of an auxiliary regulated load that may be utilized to temporarily force specifically defined forms of the battery's current curve under particular conditions, which results in improving and simplifying online open circuit voltage computations. The effectiveness of the proposed technique was successfully validated through several experimental tests. The acquired findings demonstrated its efficiency with an acceptable online state of charge estimation accuracy. Typically, an estimation error of less than 2% was recorded in most tests, while the error was less than 1% when the battery's state of charge was high.

Keywords: *Auxiliary controlled load, Dynamic load, Lithium-ion battery, OCV, SoC*

Cite this paper as: Zermout, A., Belaidi, H., & Maache, A. Online estimation of state-of-charge using auxiliary load. *Journal of Energy Systems 2024; 8*(2): 101-115, DOI: 10.30521/jes.1339832

Nomenclature	
Ip	Pulse current
Is	Steady-state current
LiB	Lithium-ion Battery
OCV	Open Circuit Voltage
OCVdp	OCV drop caused by the pulse current during a pulse duration
OCVds	OCV drop caused by the steady-state current during a pulse duration
SoC	State of Charge
T	Time constant
Tp	Pulse time
Ts	Steady-state time
Vch	Charged voltage
Vd	Discharged voltage

1. INTRODUCTION

Lithium-ion batteries (LiB) are extensively utilized as a power source in many different electronic devices such as phones, tablets, and laptops due to their decreasing prices, excellent density of energy, low self-discharge, and lifespan. In addition, LiB have outstanding efficiency in charging. They lose less energy throughout the charge/discharge cycle than other battery types because of the intelligent charging algorithm implemented in their BMS (Battery Management Systems). When storing significant amounts of energy, such as in electrical vehicles (EVs) and solar energy storage systems, this is a very helpful criterion. Regardless of these advantages, a major drawback of these batteries is the risk of burning since they can endure thermal runaway, an unsupervised and self-sustaining chemical reaction in which there is an unexpected temperature rise, frequently leading the battery to rupture and let out explosive and poisonous gases and fire. Because of this possible risk, the conveyance of lithium-ion batteries (LiB) onboard aircraft is strictly regulated both nationally and worldwide. All lithium-ion cells and batteries transported onboard airplanes but not wrapped with or enclosed within equipment (UN 3480) must be handled at a State of Charge (SoC) that is equal or below to 30% of their entire capacity, according to transport rules and industry norms.

SoC is an estimation of the amount of energy left in a cell or battery; which can be described as the quantity of electrical charge contained in the cell or the battery at any time *t* in relation to the nominal electrical charge [1,2]. SoC can be one of the significant features of lithium-ion cells for efficient and secure use in different fields such as control of photovoltaic–wind–battery systems [3,4], Electrical vehicles [5–7], microgrid energy management [8-10] and numerous other applications.

In recent years, building sophisticated and clever SoC estimators for LiB has emerged as a prominent investigation topic. The major technical challenges impeding SoC advancement can be divided into three categories. The primary issue is that the battery structure is unpredictable, making precise modeling difficult. This is related to the fact that battery packs, cells, and active-materials are totally at distinct 3D dimensions, as well as temporal scale factors (e.g., aging). The second issue is that the inner climate is difficult to predict and is vulnerable to external environmental fluctuations. Expanding LiB from experimental-phase to industrial-phase manufacture reduces the association between estimated and real data, making it harder to detect the LiB's internal conditions with confidence. Lastly, the lithium-ion batteries' inconsistencies have an immediate impact on the efficiency of the LiB pack, increasing their instability. Assessment methods established for smaller lithium-ion cells are obsolete on extensive lithium-ion batteries (e.g., LiB for electrical cars), thus estimating the SoC of a LiB or cell is very hard. As a result, better SoC approaches are urgently needed to address these difficulties [11].

Modeling allows us to comprehend more about battery behavior and assists in optimizing system efficiency and effectiveness. Battery models can be used to define V-I characteristics, SoC status, and the size of the battery. Therefore, several models were investigated to imitate the dynamic properties of the battery such as: (i) Electrical equivalent models, where single or multiple parallel pairs of resistance, capacitance, and additional circuit components are used to build an electric circuit that mimics the dynamic features of Lithium-ion batteries [12]. Moreover, PSO (Particle Swarm Optimization), GA (Genetic Algorithms), and ABC (Artificial Bee Colony) have been studied to predict the potential difference in the battery's output poles using the OCV method [13]. Based on the comparisons presented in [13], the ABC algorithm has demonstrated the best performance in OCV prediction operations. After ABC, the PSO algorithm demonstrated satisfactory outcomes. The GA with the quickest reaction time was unable to demonstrate the anticipated level of success. In the end, it was discovered that the ABC algorithm is the best approach when quick processing times and successful outcomes are required (ii) The potential difference of the battery poles is expressed using mathematical expressions of the SoC and the current in empirical models. An empirical model illustrates the basic complex features of a cell using mathematical equations or polynomials of reduced order [14]. (iii) The electrochemical model

(EM) is developed based on electrochemical processes rate and the charge exchange mechanism to describe the inner reactions within the battery. This model is the basis for several physical principles, including Faraday's first rule, Ohm's rule, diffusion rule of Fick, and the Butler-Volmer formula. The EM is written in the form of nonlinear PDEs (Partial Differential Equations). To improve the application of the electrochemical-model, a model with acceptable simulation reliability for activation frequencies ranging from 10 MHz to 1 kHz is constructed [15]. Hence, there exist many techniques for the estimation of SoC naming: Coulomb-counting [16,17], open-circuit-voltage (OCV) [18,19], Model-based method [20], impedance spectroscopy [20,21], Kalman-filter [22,23], data-driven models [24,25], etc. Each of these strategies has benefits and drawbacks, and still, more investigation is required.

Coulomb counting is one of the simplest and most effective ways to estimate SoC; however, it might suffer from drift caused by errors in current measurement and must be recalibrated from time to time. One of the calibration methods is OCV which is defined by reading the OCV after letting the battery at repose for a few hours and then mapping that voltage to SoC using a predefined lookup table. Yet, this method involves the battery being at repose (offline) for an extended duration, which is not a favored option for many applications. Online OCV estimation is possible, and some online OCV estimate algorithms by adopting a certain ECM (Equivalent-Circuit-Model) were offered for estimating SoC in the literature, which processes the real-time current and voltage of the load using KF (Kalman-Filter), RLS (Recursive-Least-Squares), and EKF (Extended-Kalman-Filter) [26–28]. However, the online OCV estimation is computationally complex and can be challenging with the existing methods because, in most applications, the load current, and voltage cannot be easily predicted or tracked effectively due to its drastic variations. The proposed method in this paper is to add an auxiliary controlled load, which can be employed to get a known predefined shape of the current curve under some conditions (for instance, during the test, the dynamic load current cannot exceed a certain level) that will help to facilitate the online OCV calculations. The proposed technique is explained in the paper's context. A test bench is used, and a number of tests were performed as real typical scenarios to validate the approach's accuracy.

The paper is structured as follow: The suggested OCV estimation approach is explained in details in Section 2. Results and discussion are outlined in Section 3. Whereas, section 4 contains the conclusions and upcoming research directions.

2. THE PROPOSED OCV ESTIMATION TECHNIQUE

As mentioned in the previous section, several existing methods can be used to compute the OCV of LiB to estimate the state of charge; however, implementing these methods can be challenging and complex, and they may not be suitable for all load conditions. To remedy these issues our proposed OCV estimation technique suggests employing the setup shown in Fig. 1(a) to temporarily force the battery's current to take on a predefined shape. The main load of the system is the dynamic load such as home, microgrid, or any other systems where their current cannot be predicted; hence, an auxiliary-controlled load is added. Therefore, the battery current can be controlled, as it will be the sum of the current consumed by both loads as expressed by Eq. (1):

$$I_{battery} = I_{dynamic} + I_{controlled} \quad (1)$$

Calculating the battery's model parameters shown in Fig. 1(b) will become straightforward and easy, as the battery's current can be adjusted to be of a suitable shape as depicted in Fig. 2. As a result, the OCV can be found; then, it is possible to estimate the state of charge (SoC) of the battery. However, this approach is not continuous, meaning that except for the period when the controlled load is activated to provide the required current shape, the SoC cannot be obtained regularly. Therefore, as illustrated in Fig. 3, it is preferable to be used to calibrate the coulomb counting method to overcome the problems of

initial SoC and accumulated error. Every aspect of this approach will be thoroughly explained in the later sections.

2.1. Test Set-up

Our method relies on the first order equivalent circuit model of the lithium-ion [7] illustrated in Fig. 1(b), the model time constant is assumed to be less than 100s according to Table 1 [7].

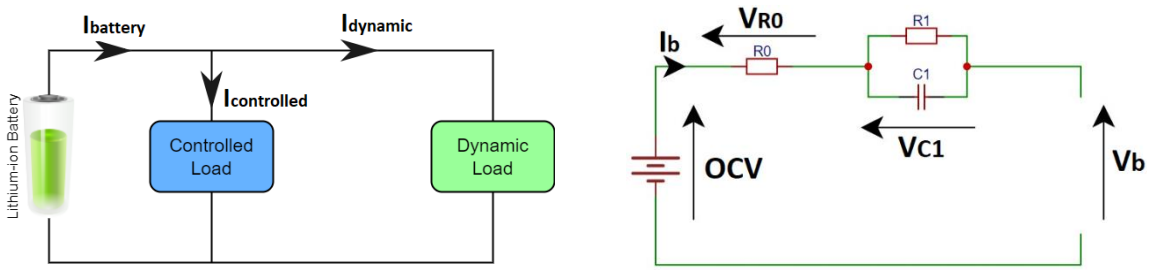

(a) (b)

Figure 1. The proposed circuits: (a) Dynamic load with the auxiliary controlled load. (b) Equivalent circuit of first-order RC model.

Table1. Lithium-ion 1-RC model time constant for different SoC [7].

State-of-Charge	τ_1 *in s*	R_1 *in* Ω	C_1 *in* 10^3 *F*
0	56.2430	0.0382	1.4743
0.05	42.8082	0.0263	1.6265
0.1	51.3875	0.0226	2.2758
0.15	47.5964	0.0244	1.9491
0.2	55.9597	0.0237	2.3622
0.3	34.7826	0.0203	1.7126
0.4	35.8938	0.0204	1.7612
0.5	41.9287	0.0211	1.9919
0.6	37.5657	0.0267	1.4049
0.7	40.6504	0.0242	1.6798
0.8	38.5654	0.0272	1.4178
0.9	37.3134	0.0235	1.5878
1	46.2321	0.0240	1.9287

Fig. 2 depicts the fundamental operation of this approach. In a normal operating condition, the controlled load should be OFF and the battery's current will match the dynamic load current, which may fluctuate excessively. Whenever it is required to determine the OCV, the controlled load is turned ON. Consequently, the battery's current is adjusted to get the required form as illustrated. The specifications of the chosen current form are as follows: First, the current is fixed to the value I_s for T_s duration, which will bring the capacitor *C1* to a steady state. Then, the I_p current pulse will be applied for T_p duration. After that, the current will be set to the value I_s for another T_p period. Finally, the controlled current load will be turned OFF, and the battery's current will be equal to the dynamic load again. The purpose of this controlled current pattern is that it will induce a specific battery voltage response, which will facilitate the online OCV calculation.

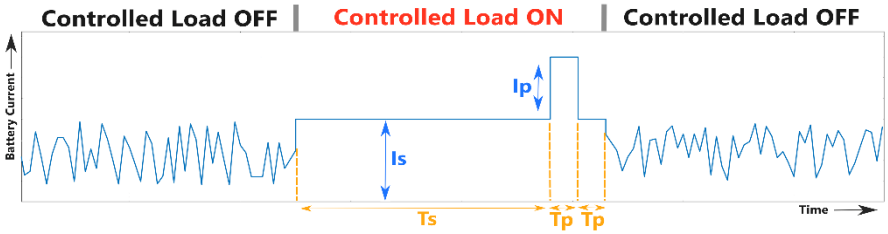

Figure 2. The fundamental operation of the controlled load approach.

Fig. 3 summarizes the working mechanism of this proposed method. As an application example, this method can be used with the Coulomb counting technique to calibrate or set its initial SoC and omit the occurring drift. First, the system reads the instantaneous battery's current and the actual SoC that was tracked using Coulomb counting. If the SoC is very low or the battery's current is high, the recalibration should not be performed. Otherwise, the different current form parameters I_s, I_p, T_s, and T_p are set, and then the controlled load is turned on to apply the predefined current shape. It is worth noting that the dynamic current should be equal to or less than the current *Is*. However, if the dynamic load current suddenly rises above the current I_s, the desired current shape for calculating the OCV will be distorted. In this case, the OCV estimation process will stop, the controlled load will be turned off, and the whole process will be restarted from the beginning.

On the other hand, if the estimation process is completed successfully during the predefined timeline; then, the controlled load current will become zero, and the online OCV can be calculated using the proposed method that will be described later. Thus, the SoC can be obtained using the OCV-SoC lookup table mapping and finally, the Coulomb counting SoC can be recalibrated. This process can be repeated periodically when recalibration is required.

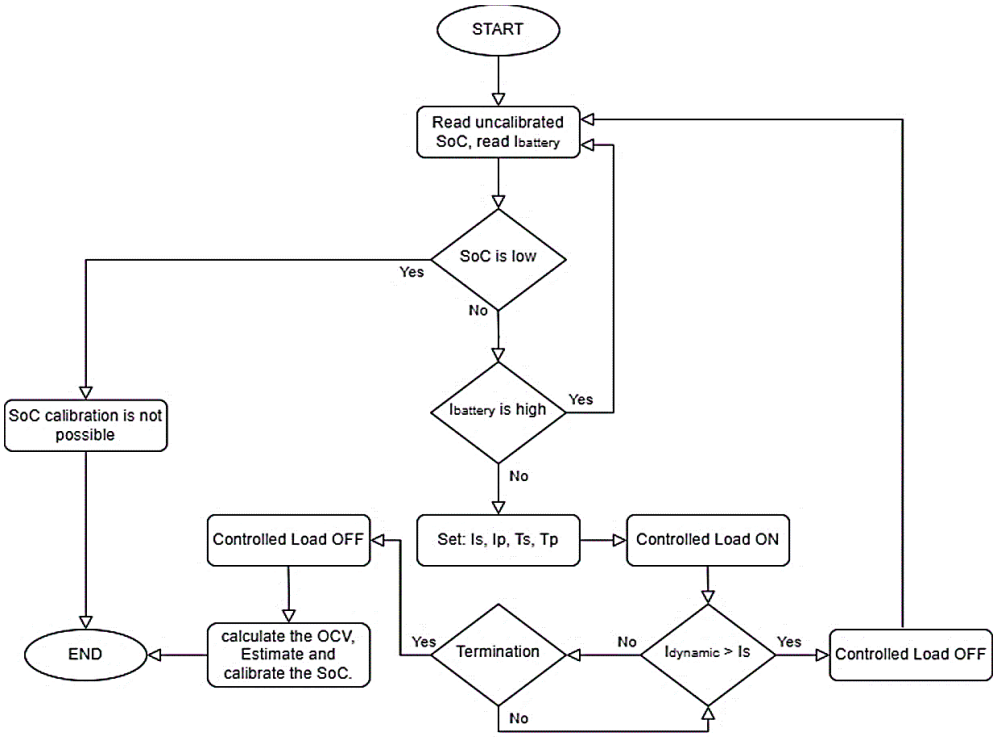

Figure 3. Flowchart representing the working mechanism of the proposed technique.

For the validation of the proposed technique, illustration tests of real scenarios were performed on an old LiB. Fig. 4 demonstrates the process of calculating the online OCV as clarified in Section 2.2 in addition to investigating the ability of the method to get the true OCV, and also extracting the relationship between the estimated OCV and an actual two hours OCV.

From time *0* to *500 s*, the battery's current is random and less than *500 mA*, similar to the dynamic load's current. After that, the current is fixed to $I_s = 500\ mA$ for $Ts=500\ s$ from the time *500 s* to *1000 s*, in order to mimic the controlled load usage (see Fig. 2) Then, at time *1000s*, a current pulse $I_p = 300\ mA$ was added with pulse time $T_p = 30\ s$. At *1030 s* the current was forced to I_s again for the duration *Tp*. Finally, at *1060 s*, the battery's current is *0A*. In a real application, after the estimation of OCV, the controlled load current becomes *0 A*, and the battery current will be equal to the dynamic load current. However, in the performed test scenario, the battery was disconnected for *two hours* to get its true OCV and compare it to the OCV obtained using the proposed method.

The parameters I_s, T_s, I_p, and T_p can be set to different values (in a real application, I_s should always be superior to the dynamic load current). However, for experimental purposes, these parameters were set to *500 mA*, *500 s*, *300 mA*, and *30 s*, respectively. Fig. 5(a) illustrates the points used for the online OCV calculation method.

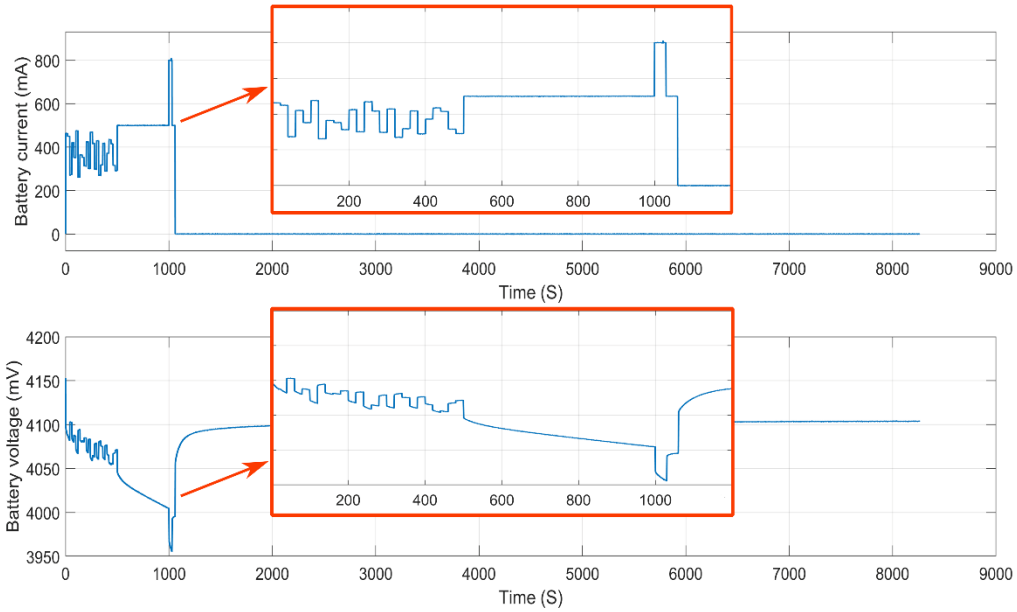

Figure 4. Conducted test for the OCV calculation.

2.2. OCV Calculation

To calculate the OCV online, the model parameters shown in Fig. 1(b) must be known. The voltage *VC1*, illustrated in Fig. 5(b) is assumed equivalent to the voltage across *C1* shown in Fig. 1(b) of the lithium-ion equivalent circuit model during the current pulse *Ip* seen in Fig. 4 at time *1000 s*. Whereas, the voltages V_{ch} and V_d should be extracted from the battery voltage response using the specific point presented in Fig. 5(a).

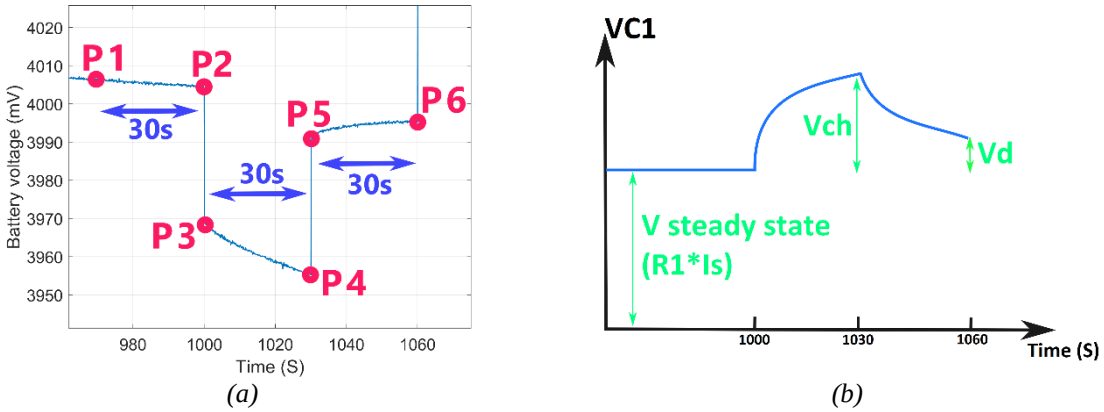

(a) *(b)*

Figure 5. Zoomed-in voltage of the test: (a) Illustration of the points used for the OCV calculation. (b) Illustration of voltage charging and discharging assumed curve shape of C1 during the test.

First, the battery voltage response shown in Fig. 5(a) contains an OCV drop caused by the discharging current. Therefore, to extract the *VC1* changes, the OCV drop during the current I_s and during the current (I_s+I_p) must be calculated and filtered out. Since the current was *500 mA* for *500 s*, the capacitor C_1 can be assumed to be at its steady state voltage, at the last 30 s of the period *Ts=500 s*. Thus, the battery voltage drop from *970 s* to *1000 s* (see Fig. 5(a)) can be considered purely the OCV drop. It is expressed by Eq. (2), where OCV_{ds} signifies the OCV drop caused by the I_s current in 30 seconds, and OCV_{dp}

signifies the OCV drop when the current I_p is added within the same 30 seconds. V_{p1} and V_{p2} define the voltages at the points P_1 and P_2, respectively; and so on as expressed by Eq. (1):

$$OCV\text{ds} = Vp1 - Vp2 \tag{2}$$

Then, the OCV drop per *30 s* after adding the current pulse at *800 mA* (I_s+I_p) must be calculated within the period from *1000 s* to *1030 s*. Assuming that the OCV drop rate per current is constant during the test, so it can be calculated using Eq. (3):

$$OCV\text{dp} = OCV\text{ds}\ (Is + Ip)/Is \tag{3}$$

When the pulse I_p = *300 mA* is applied once the current reaches *500 mA*, the capacitor can be considered in the charging phase, as shown in Fig. 5(b). The charged voltage V_{ch} can be considered as the difference between V_{p3} and V_{p4} minus OCV_{dp} as given by Eq. (4):

$$Vch = Vp3 - Vp4 - \ OCV\text{dp} \tag{4}$$

Whereas, the discharged voltage V_d is calculated using Eq. (5) (see Fig. 5(b)):

$$Vd = \ Vch - (Vp6 - Vp5 + \ OCV\text{ds}) \tag{5}$$

The C_1 charging equation can be expressed by Eq. (6) as follow:

$$Ip\ R1\ \left(1 - e^{-\frac{Tp}{T}}\right) = \ Vch \tag{6}$$

Whereas, the discharging equation can be written in Eq. (7) as follow:

$$Vd = \ Vch\ e^{-\frac{Tp}{T}} \tag{7}$$

Therefore, from Eq. (7) the time constant T can be extracted by Eq. (8):

$$T = \ -Tp/\ln\left(\frac{Vd}{Vch}\right) \tag{8}$$

Then, T can be substituted in Eq. (6) to calculate $R1$ as explained in Eq. (9)

$$R1 = \frac{Vch}{Ip\left(1 - e^{-\frac{Tp}{T}}\right)} \tag{9}$$

and R_0 extracted by Eq. (10):

$$R0 = \frac{Vp2 - Vp3}{Ip} \tag{10}$$

Finally, the estimated OCV can be calculated at P_2 using Eq. (11) based on the model given in Fig. 1(b) where OCV=V_b+V_{R0}+V_{C1}; by assuming that V_{C1} is in its steady state.

$$OCV@P2 = \ Vp2 + (R0 + R1)\ Is \tag{11}$$

Hence, the OCV in this test is calculated at *P6* using Eq. (12). This value will later be compared to the two hours OCV.

$$OCV@P6 = OCV@P2 - OCV_{dp} - OCV_{ds} \quad (12)$$

However, there is a voltage offset that has appeared; which needs to be added to the estimated OCV using Eq. (13):

$$OCV = OCV@P6 + offset \quad (13)$$

The above-outlined OCV calculation procedure does not involve *C1*. But, if it is needed, it can be calculated using Eq. (14):

$$C1 = \frac{T}{R1} \quad (14)$$

3. RESULTS AND DISCUSSION

3.1. Test Equipment

All the validation tests and experiments outlined in the paper were conducted on an aged lithium-ion battery cell, which has the characteristics reported in Table 2.

Table 2. Characteristics of the used LiB cell

Producer	Type	Nominal capacity	Max voltage	Mini voltage
LG	LGABD18650	3000 mAh	4.35V	3.0V

Fig. 6 provides a representation of the test bench that was utilized for the tests. It has already been used in previous work for battery characterization [29]. The ESP32 is the central controller entity that manages both Relay1 and Relay2 for the charging and discharging path. Moreover, it also controls the current intensity through the charging or discharging transistor. The ADS1115 is a 16-bit 2's complement ADC that reads the battery voltage and the shunt resistor voltage to get the current's value. It also measures the temperature values and then sends the data to the ESP32, which transmits it to the computer to be stored and processed. Furthermore, a separate heating chamber can be used. The test bench characteristics and performance are summarized in Table 3.

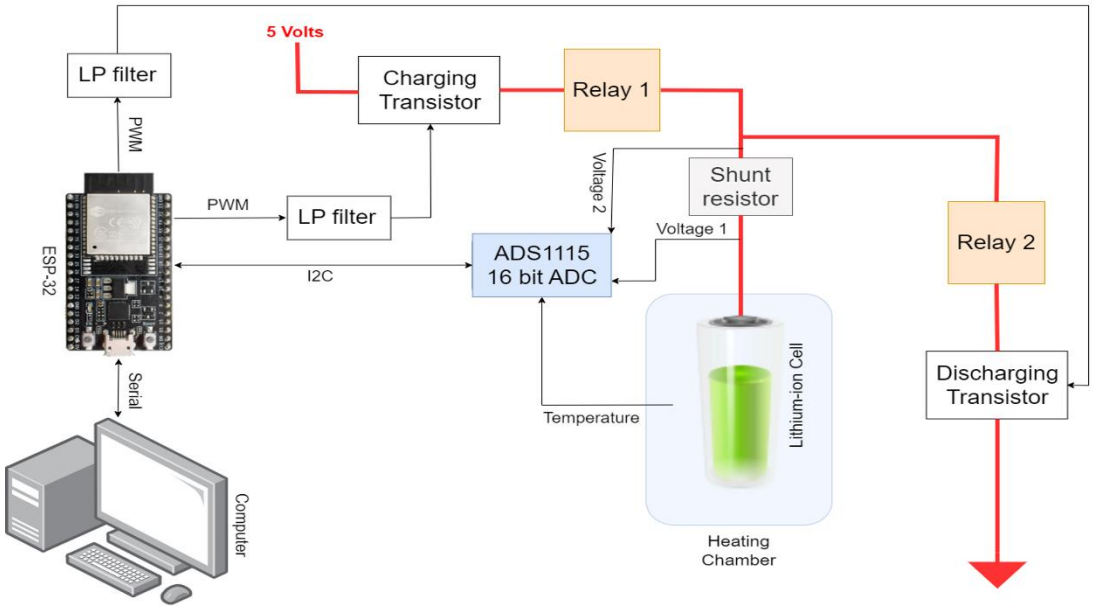

Figure 6. Battery test bench diagram used in this work [29].

Table 3. The test bench performances

Voltage accuracy	Current accuracy	Configured sampling rate	Max voltage	Maximum current	Load hysteresis at *1A*	Voltage error	Current error
0.187mA	0.153mA	10 Samples/S	5V	5A	<3.5mA	0.6mV	<1.2%

3.2. Results and Discussion

Fig. 7 highlights the results obtained from the tests outlined in Fig. 4. These tests were conducted to determine the best correlation between the online estimated OCV values and the true OCV values after two hours rest of the LiB.. These tests are performed repeatedly at different SoC within a complete discharge cycle at room temperature (around *23°C*). The error of the estimated OCV compared to the *two hours* OCV is consistent. The resulting error can be minimized by adding an offset of *13.82 mV* (the average error) to the estimated value of OCV. The *two hours* OCV, the estimated OCV, and the estimated OCV with the offset are shown in Fig. 7. When comparing the *two hours* OCV with the (estimated OCV with offset), the error is very low; in some points, the plots are almost superimposed. The error, in general, does not exceed *8 mV* except for one error spike of *15.7 mV* where the SoC is around *0.63*. In addition, when the SoC is very small, the error is high.

As it can be noticed, in the last tests where SoC is less than *0.2*, the error is not consistent. This can be due to the rapid drop rate change of the battery OCV. Hence, this method is not recommended at low SoC.

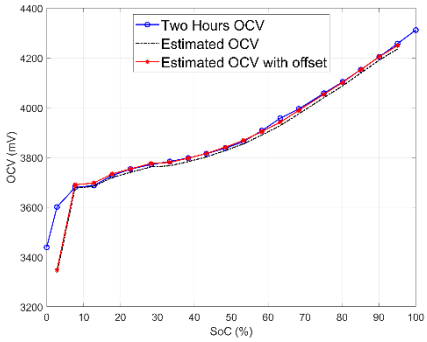

Figure 7. Comparison between the two hours OCV, Estimated OCV, and Estimated OCV with offset.

Furthermore, various additional tests were performed, not just to evaluate the accuracy of the online OCV estimation, but also to validate the accuracy of the discussed method to estimate the SoC. Although the graph in Fig. 7 can be used with the next tests to map the OCV to the SoC, an additional test was performed to extract OCV versus SoC with better resolution. First, the battery was fully charged; thereafter, it was discharged by 4% of its total capacity using a 500-mA constant current. Secondly, the battery is left at rest for two hours before recording its OCV. Finally, these steps are carried out repeatedly until the battery is completely discharged; the obtained OCV versus SoC relations is recorded in Fig. 8.

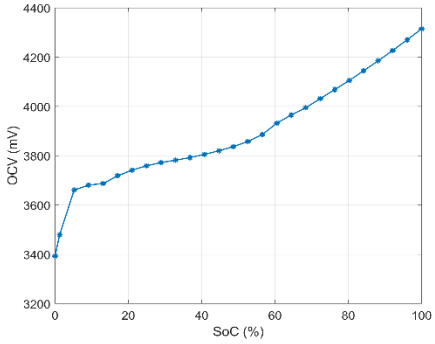

Figure 8. OCV versus the SoC of the used LiB.

As stated before, our proposed method cannot be used continuously to estimate the SoC. Therefore, the predefined pulse can only be used whenever calibration is needed. However, for experimental purposes, the LiB was fully charged and then completely discharged continuously (without rest) in order to assess the performance of the proposed method for different SoC levels. The experiment involved using a fixed current of 500mA with a current pulse of 300 mA for 30 seconds at each 500 seconds interval as illustrated in Fig. 9. This test was performed at room temperature (around 23°C) on the same battery used in previous tests.

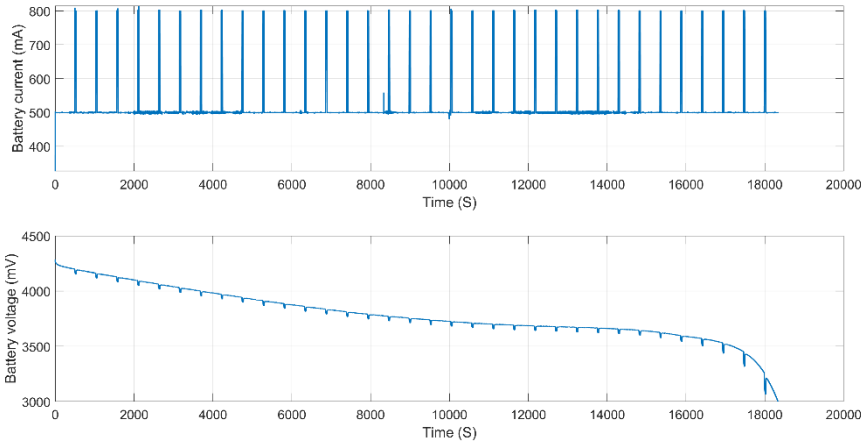

Figure 9. Test to calculate the Battery's SoC.

As can be noticed in Fig. 9, each current pulse during the discharging process had a corresponding battery voltage response exactly as explicated before. Thus, the OCV can be calculated at each pulse using the equations Eq. (2) to Eq. (13). Moreover, the obtained OCV can be mapped to the SoC using the lookup table plotted in Fig. 8. As a reference, the true SoC was tracked using the Coulomb-counting technique; thus, the SoC estimation and the Coulomb-counting SoC were compared and the related error is plotted in Fig. 10. The error is smaller than 1% when the battery SoC is more than 70%, and when SoC is between 70% and 30% the error does not exceed 2%. However, when the battery is under 30%, the error starts exceeding 6%.

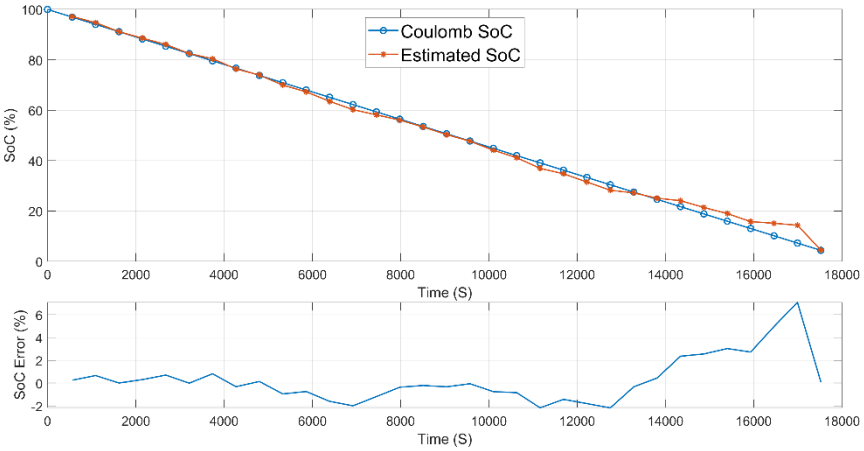

Figure 10. The estimated SoC vs the Coulomb counting SoC.

The equivalent circuit model's parameters during the test in Fig. 9 are calculated using the same equations used for the OCV estimation and they are demonstrated in Fig. 11. It can be clearly noticed that when the SoC drops under 30%, the model parameters shift drastically. This trend may cause the incompatibility of the equivalent circuit model with the battery behavior, which leads to inaccuracy in the online OCV estimation; and thus, a big error in SoC estimation.

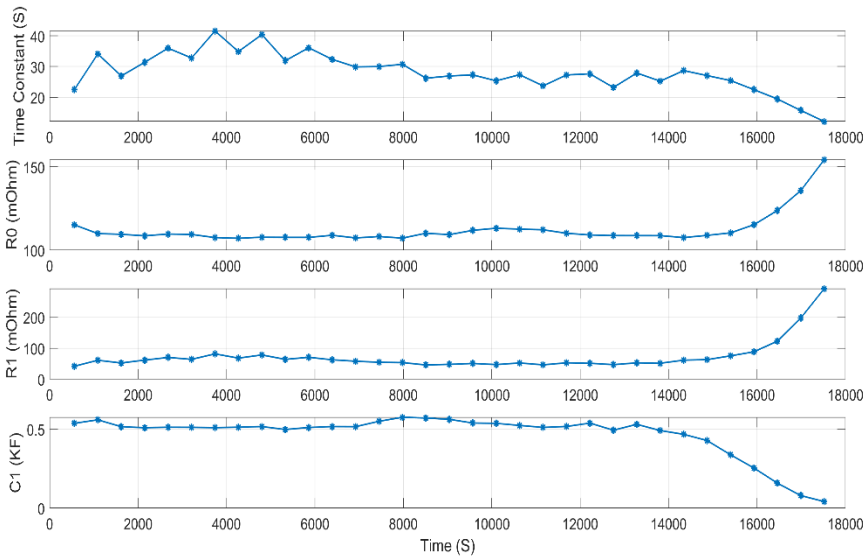

Figure 11. 1st order RC equivalent circuit model parameters.

Moreover, another test was conducted similar to the one illustrated in Fig. 9; but this time the battery was put inside a heated chamber at 40°C (as illustrated in Fig. 12).

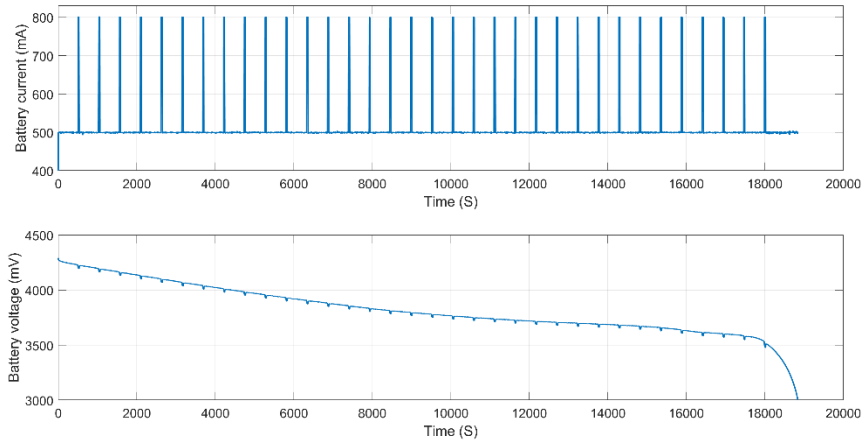

Figure 12. Test to calculate the Battery's SoC at 40°C.

The battery's SoC was then obtained following the same way as before. The new results are shown in Fig. 13. Surprisingly, the error is less than 1% when the SoC is more than 35%, and when the SoC is less than 35% the error does not exceed 3.5%. Thus, this method is not affected when the temperature changes from around 23°C to 40°C. At each test instance, the Coulomb counting SoC was calculated by dividing the discharged capacity at each time over the total discharged capacity of the test.

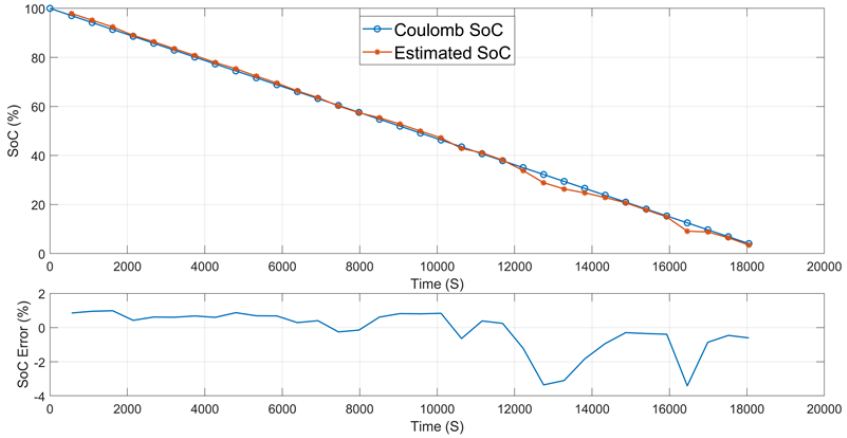

Figure 13. Comparison of the estimated SoC and the Coulomb counting SoC at 40°C.

A final test was conducted exactly the same way as the two previous tests with only one difference, which is changing I_s to 800 mA. The final test process is shown in Fig. 14. This test was performed at a room temperature of around 23°C. Once the discharging is completed, the current was set to 500 mA to get the same depth of discharge as the previous similar tests.

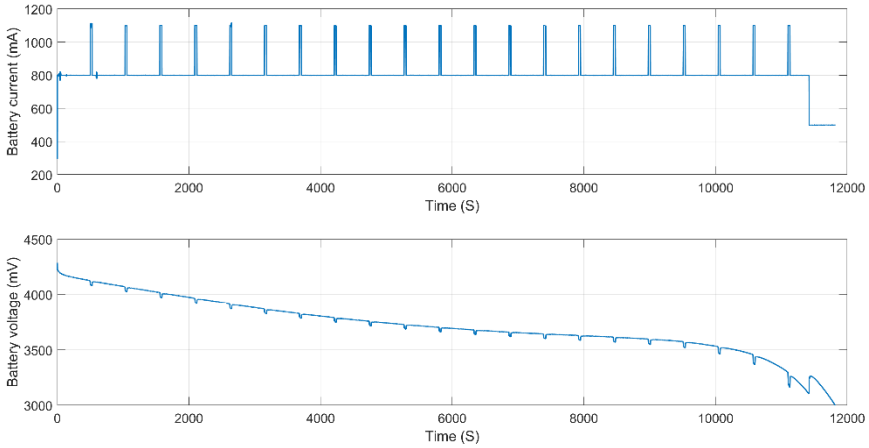

Figure 14. Test to calculate the Battery SoC at 23°C with I_s= 800 mA.

By changing I_s to 800 mA in this test, the measured error was too big exceeding 15%, as presented in Fig. 15. Although this could be an issue, the error can be smaller as before by setting the offset to 69.5 mV instead of 13.82 mV, as shown in Fig. 16. Thus, each parameter value I_s or I_p should have its corresponding predetermined offset.

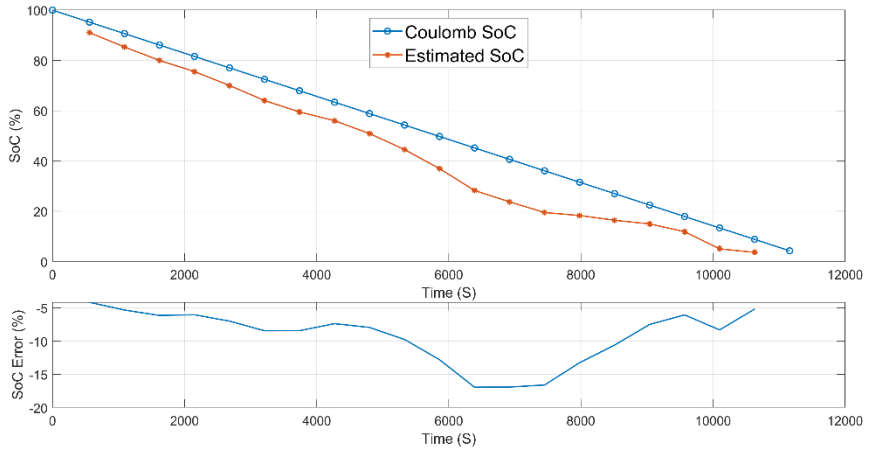

Figure 15. The estimated SoC vs Coulomb counting SoC with Is=800 mA.

As can be seen in Fig. 16, after modifying the offset in calculating the OCV in Eq. (13), the error becomes less than 1% when the battery SoC is more than 75%, and 2.25% or less when SoC is between 30% and 75%. When the SoC of the battery is low, the error goes larger than 4%. It can be deduced from the performed SoC tests that the change in temperature from 23°C to 40°C does not affect the SoC precision. However, by changing the I_s current during the controlled load intervention scenario, a considerable error occurs. Thus, a change in the offset to the right value corresponding to I_s is necessary to minimize the error.

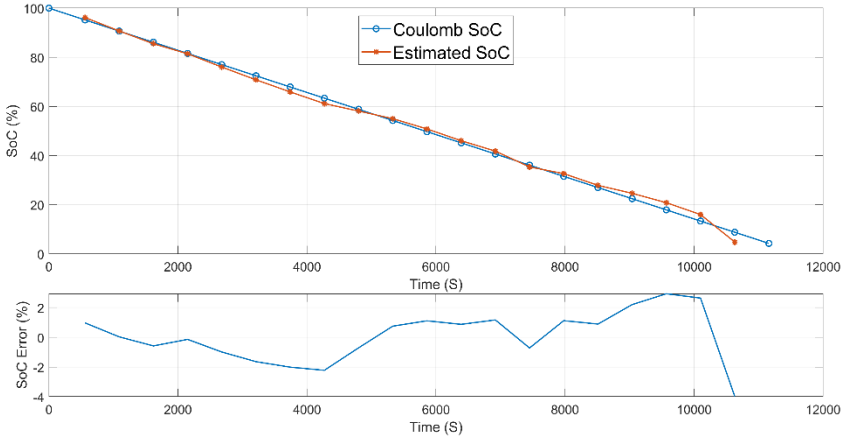

Figure 16. The estimated SoC vs the Coulomb counting SoC with Is=800mA, after adjusting the offset to 69.5mA.

3.3. Comparison

Fig. 17 summarizes the obtained results throughout our study and then compares them to some existing work in the literature. The conducted test results demonstrate that the suggested approach has good precision when it is used at SoC levels above 35%, with an average error that does not exceed 1%, and a maximum error of less than 2.5%. Furthermore, if this method is used only when SoC is above 75% it will provide an SoC estimation with an error of less than 1%, compared with the results obtained by [26] where the authors worked with a similar method and stated SoC error less than 2%. Whereas, in the review paper [30], a comparison between recent hybrid methods and recent deep learning algorithms was shown. Generally, the different methods were declared with an average error ranging from 1% up to 6%. According to the analysis extracted in [30], the work of [31] has revealed the minimum error for hybrid methods and [32] has exposed the smallest error concerning deep learning algorithms. Therefore, our obtained results were compared to these two former references ([31] and [32]). Generally, our developed method error is better with an average of less than 1% under (23°C) and especially when used with SoC higher than 75%. Moreover, [30] concluded the review by stating that the existing methods can estimate the SOC at varying temperatures with an average error within 3.5% and works under untrained temperatures; whereas, our obtained average error didn't exceed 1% even under 40°C.

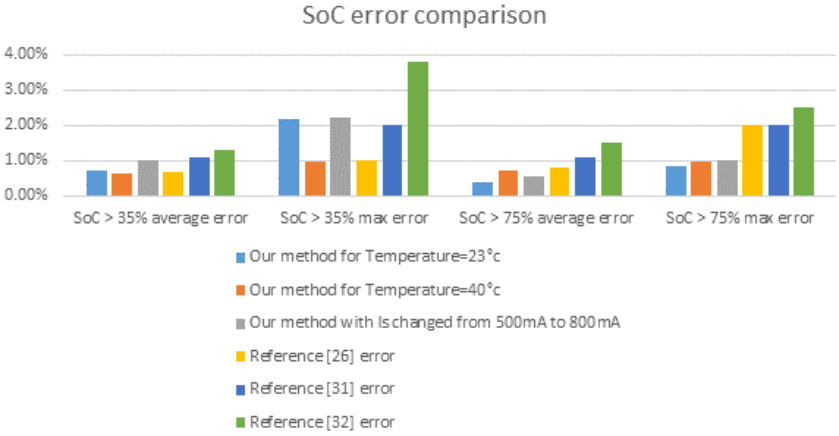

Fig. 17. Comparison between our methods and recently developed methods.

4. CONCLUSION AND PERSPECTIVES

This paper described the development of an online OCV estimation method, which is based on temporarily forcing a predefined current curve using an auxiliary controlled load. This novel technique can be an ideal solution for calibrating Coulomb counting method and setting its initial SoC value. The obtained results were acceptable with an estimation error typically less than 2%. When employed at high SoC, the results improve even further to less than 1%, even with the low performance of the battery test system in use since some drift in the current sensor was observed. The potential advantages of the proposed method are its simplicity and low computational complexity. Moreover, it obtains the parameters of the equivalent circuit model online, which enhances the accuracy, and reliability. Furthermore, it is not affected by aging and temperature; since, it has been shown that the SoC precision is unaffected by a temperature shift from 23°C to 40°C.

Concerning future work vision, our objective is to re-conduct all tests with a sophisticated shunt resistor on a calibrated and high-performance battery test bench system that can produce better results. The approach can also be implemented to target a real application. The work can also include tests under variable temperatures and estimating the OCV with a 2-RC equivalent circuit model or any other model. Furthermore, more tests will be carried out for better current curves' parameters and shapes to get optimal performances.

REFERENCES

[1] Espedal IB, Jinasena A, Burheim OS, Lamb JJ. Current Trends for State-of-Charge (SoC) Estimation in Lithium-Ion Battery Electric Vehicles. *Energies* 2021; *14*(11):3284. doi:10.3390/en14113284.
[2] Abdi H, Mohammadi-ivatloo B, Javadi S, Khodaei AR, Dehnavi E. Energy Storage Systems. In: Distributed Generation Systems. Elsevier; 2017:333-368. doi:10.1016/B978-0-12-804208-3.00007-8.
[3] Azaroual M, Ouassaid M, Maaroufi M. Model predictive control-based energy management strategy for grid-connected residential photovoltaic–wind–battery system. In: Renewable Energy Systems. Elsevier; 2021:89-109. doi:10.1016/B978-0-12-820004-9.00014-0.
[4] Uğurlu A, Gökçöl C. A case study of PV-wind-diesel-battery hybrid system. *J Energy Syst.* 2017; *1*(4):138-147. doi:10.30521/jes.348335.
[5] Wang K, Wang W, Wang L, Li L. An Improved SOC Control Strategy for Electric Vehicle Hybrid Energy Storage Systems. *Energies* 2020; *13*(20):5297. doi:10.3390/en13205297.
[6] Zhang R, Xia B, Li B, et al. State of the Art of Lithium-Ion Battery SOC Estimation for Electrical Vehicles. *Energies* 2018; *11*(7): 1820. doi:10.3390/en11071820.
[7] Zhang L, Peng H, Ning Z, Mu Z, Sun C. Comparative Research on RC Equivalent Circuit Models for Lithium-Ion Batteries of Electric Vehicles. *Appl Sci.* 2017; *7*(10): 1002. doi:10.3390/app7101002.
[8] Belaidi H, Bentarzi H, Rabiai Z, Abdelmoumene A. Multi-agent System for Voltage Regulation in Smart Grid. In: Hatti M, ed. Artificial Intelligence and Renewables Towards an Energy Transition. Vol 174. Lecture Notes in Networks and Systems. Springer International Publishing; 2021:487-499. doi:10.1007/978-3-030-63846-7_46.
[9] Belaidi H, Rabiai Z. Decentralized Energy Management System Enhancement for Smart Grid: In: Management Association IR, ed. Research Anthology on Smart Grid and Microgrid Development. *IGI Global* 2022, 77-90. doi:10.4018/978-1-6684-3666-0.ch004.
[10] Kaddour D, Belaidi H. Impact of Integrating DERs and ESS on Smart-Grid Supply Continuity: A Review. In: 2022 3rd International Conference on Human-Centric Smart Environments for Health and Well-Being (IHSH); 26-28 October 2022: IEEE, 7-12. doi:10.1109/IHSH57076.2022.10092035.
[11] Hu X, Cao D, Egardt B. Condition Monitoring in Advanced Battery Management Systems: Moving Horizon Estimation Using a Reduced Electrochemical Model. *IEEEASME Trans Mechatron* 2018; *23*(1): 167-178. doi:10.1109/TMECH.2017.2675920.
[12] Thakkar RR. Electrical Equivalent Circuit Models of Lithium-ion Battery. In: E. Okedu K, ed. Management and Applications of Energy Storage Devices. IntechOpen; 2022. doi:10.5772/intechopen.99851.
[13] Çarkit T, Alçi M. Comparison of the performances of heuristic optimization algorithms PSO, ABC and GA for parameter estimation in the discharge processes of Li-NMC battery. *J Energy Syst.* 2022; *6*(3): 387-400. doi:10.30521/jes.1094106.

[14] Meng J, Luo G, Ricco M, Swierczynski M, Stroe DI, Teodorescu R. Overview of Lithium-Ion Battery Modeling Methods for State-of-Charge Estimation in Electrical Vehicles. Appl Sci. 2018; *8*(5): 659. doi:10.3390/app8050659.
[15] Zhang Q, Wang D, Yang B, Cui X, Li X. Electrochemical model of lithium-ion battery for wide frequency range applications. Electrochimica Acta. 2020; *343*: 136094. doi:10.1016/j.electacta.2020.136094.
[16] Ng KS, Moo CS, Chen YP, Hsieh YC. Enhanced coulomb counting method for estimating state-of-charge and state-of-health of lithium-ion batteries. *Appl Energy* 2009; *86*(9): 1506-1511. doi:10.1016/j.apenergy.2008.11.021.
[17] Chang WY. The State of Charge Estimating Methods for Battery: A Review. *ISRN Appl Math.* 2013; *2013*: 1-7. doi:10.1155/2013/953792.
[18] Dong G, Wei J, Zhang C, Chen Z. Online state of charge estimation and open circuit voltage hysteresis modeling of LiFePO4 battery using invariant imbedding method. *Appl Energy* 2016; *162*: 163-171. doi:10.1016/j.apenergy.2015.10.092.
[19] Zheng F, Xing Y, Jiang J, Sun B, Kim J, Pecht M. Influence of different open circuit voltage tests on state of charge online estimation for lithium-ion batteries. *Appl Energy* 2016; *183*: 513-525. doi:10.1016/j.apenergy.2016.09.010.
[20] Meng J, Ricco M, Luo G, et al. An Overview and Comparison of Online Implementable SOC Estimation Methods for Lithium-Ion Battery. *IEEE Trans Ind Appl.* 2018; *54*(2): 1583-1591. doi:10.1109/TIA.2017.2775179.
[21] Wang X, Wei X, Dai H, Wu Q. State Estimation of Lithium Ion Battery Based on Electrochemical Impedance Spectroscopy with On-Board Impedance Measurement System. In: 2015 IEEE Vehicle Power and Propulsion Conference (VPPC); 19-22 October 2015: IEEE, 1-5. doi:10.1109/VPPC.2015.7353021.
[22] Spagnol P, Rossi S, Savaresi SM. Kalman Filter SoC estimation for Li-Ion batteries. In: 2011 IEEE International Conference on Control Applications (CCA); 28-30 September 2011: IEEE, 587-592. doi:10.1109/CCA.2011.6044480.
[23] Rzepka B, Bischof S, Blank T. Implementing an Extended Kalman Filter for SoC Estimation of a Li-Ion Battery with Hysteresis: A Step-by-Step Guide. *Energies* 2021; *14*(13): 3733. doi:10.3390/en14133733.
[24] Ali M, Kamran M, Kumar P, et al. An Online Data-Driven Model Identification and Adaptive State of Charge Estimation Approach for Lithium-ion-Batteries Using the Lagrange Multiplier Method. *Energies* 2018; *11*(11):2940. doi:10.3390/en11112940.
[25] Wang Y, Yang D, Zhang X, Chen Z. Probability based remaining capacity estimation using data-driven and neural network model. *J Power Sources* 2016; *315*: 199-208. doi:10.1016/j.jpowsour.2016.03.054.
[26] Xiong R, Yu Q, Wang LY. Open circuit voltage and state of charge online estimation for lithium ion batteries. *Energy Procedia* 2017;*142*:1902-1907. doi:10.1016/j.egypro.2017.12.388.
[27] Song Y, Park M, Seo M, Kim SW. Online State-of-Charge Estimation for Lithium-Ion Batteries Considering Model Inaccuracies Under Time-Varying Current Conditions. *IEEE Access* 2020; *8*: 192419-192434. doi:10.1109/ACCESS.2020.3032752.
[28] Meng J, Boukhnifer M, Diallo D. Comparative study of lithium-ion battery open-circuit-voltage online estimation methods. *IET Electr Syst Transp.* 2020; *10*(2): 162-169. doi:10.1049/iet-est.2019.0026.
[29] Zermout A, Belaidi H, Maache A. Implementation of Battery Characterization System. *Eng. Proc.* 2023; 29(1): 12. https://doi.org/10.3390/engproc2023029012
[30] Girijaprasanna, T., & Dhanamjayulu, C. (2022). A review on different state of battery charge estimation techniques and management systems for EV applications. Electronics, 11(11), 1795.
[31] LI, Jiabo, YE, Min, GAO, Kangping, et al. SOC estimation for lithium-ion batteries based on a novel model. IET Power Electronics, 2021, vol. 14, no 13, p. 2249-2259.
[32] Yang, F., Li, W., Li, C., & Miao, Q. (2019). State-of-charge estimation of lithium-ion batteries based on gated recurrent neural network. Energy, 175, 66-75.